2008-05-15

Energization-dependent endogenous activation of proton conductance in skeletal muscle mitochondria

Parker, N

10.1042/bj20080006
Biochemical Journal
Portland Press Ltd.

BJ www.biochemj.org

BJ Energy

Biochem. J. (2008) **412**, 131–139 (Printed in Great Britain) doi:10.1042/BJ20080006

Energization-dependent endogenous activation of proton conductance in skeletal muscle mitochondria

Nadeene PARKER*†[1], Charles AFFOURTIT*, Antonio VIDAL-PUIG† and Martin D. BRAND*

*MRC Dunn Human Nutrition Unit, Hills Road, Cambridge CB2 0XY, U.K., and †Metabolic Research Laboratories, Level 4, Institute of Metabolic Science, Box 289, Addenbrooke's Hospital, Cambridge CB2 0QQ, U.K.

Leak of protons into the mitochondrial matrix during substrate oxidation partially uncouples electron transport from phosphorylation of ADP, but the functions and source of basal and inducible proton leak *in vivo* remain controversial. In the present study we describe an endogenous activation of proton conductance in mitochondria isolated from rat and mouse skeletal muscle following addition of respiratory substrate. This endogenous activation increased with time, required a high membrane potential and was diminished by high concentrations of serum albumin. Inhibition of this endogenous activation by GDP [classically considered specific for UCPs (uncoupling proteins)], carboxyatractylate and bongkrekate (considered specific for the adenine nucleotide translocase) was examined in skeletal muscle mitochondria from wild-type and *Ucp3*-knockout mice. Proton conductance through endogenously activated UCP3 was calculated as the difference in leak between mitochondria from wild-type and *Ucp3*-knockout mice, and was found to be inhibited by carboxyatractylate and bongkrekate, but not GDP. Proton conductance in mitochondria from *Ucp3*-knockout mice was strongly inhibited by carboxyatractylate, bongkrekate and partially by GDP. We conclude the following: (i) at high protonmotive force, an endogenously generated activator stimulates proton conductance catalysed partly by UCP3 and partly by the adenine nucleotide translocase; (ii) GDP is not a specific inhibitor of UCP3, but also inhibits proton translocation by the adenine nucleotide translocase; and (iii) the inhibition of UCP3 by carboxyatractylate and bongkrekate is likely to be indirect, acting through the adenine nucleotide translocase.

Key words: adenine nucleotide translocase, carboxyatractylate, GDP, proton leak, uncoupling protein (UCP), UCP3.

INTRODUCTION

During substrate oxidation, protons are pumped out of the mitochondrial matrix, creating an electrochemical proton gradient. This protonmotive force is used to drive ATP synthesis. However, substrate oxidation is not fully coupled to ATP synthesis; some of the electrochemical gradient is dissipated by protons leaking back into the matrix through natural proton conductance pathways across the mitochondrial inner membrane [1,2]. Mitochondrial proton leak may cause up to 25 % of the resting metabolic rate [3,4] and may still be significant when ATP turnover is high [5]. The prominence of mitochondrial proton leak suggests that it is physiologically important, and several roles have been suggested [4], including protection against mitochondrial free radical production [6] and regulation of insulin secretion in pancreatic β-cells [7].

Proton leak occurs through several pathways, some basal and some inducible. Membranes are themselves intrinsically leaky to protons [8] but proteins embedded in a bilayer can greatly increase permeability [4,9,10]. Half to two-thirds of the basal mitochondrial proton conductance is dependent upon the most abundant carrier protein in the mitochondrial inner membrane, the ANT (adenine nucleotide translocase) [11]. ANT-dependent basal proton conductance occurs even if the carrier is inhibited by carboxyatractylate, showing that this leak pathway does not require normal carrier function [11].

Unlike basal proton conductance, specific activators and inhibitors affect inducible proton conductance. Inducible conductance can be catalysed by ANT in the presence of fatty acids [12,13], AMP [14] or the lipid peroxidation product hydroxynonenal [15]. This pathway is inhibited by carboxyatractylate, bongkrekate and by the ANT substrates, ATP or ADP. It is not known to be sensitive to other nucleotides. Other mitochondrial carriers, such as the glutamate [16] and phosphate carriers [17], will catalyse proton conductance in the presence of fatty acids. Specific UCPs (uncoupling proteins) also catalyse inducible proton conductance [18–21]. The best understood is UCP1, found primarily in brown adipose tissue and specialized for adaptive thermogenesis. Proton conductance through UCP1 is activated by fatty acids [22], superoxide [23], derivatives such as hydroxynonenal [15,24] and hydroxynonenal analogues (such as retinoic acid [25]). UCP2, found in a variety of tissues [26], and UCP3, found primarily in skeletal muscle [27,28], can be activated by fatty acids [29,30], superoxide [23] and hydroxynonenal and its analogues [15].

A striking aspect of the UCPs is the inhibition of their proton conductance by a broad range of purine nucleotides. Unlike the proton conductance of the adenine nucleotide carrier, UCPs are strongly inhibited not only by ATP and ADP, but also by GTP and GDP [14]. This difference in specificity has led to widespread use of GDP as a diagnostic inhibitor of UCP function *in vitro* (e.g. [31–34]), particularly in systems that lack a UCP-ablated control [35–38].

In the present study we report an endogenous increase in the proton conductance of skeletal muscle mitochondria incubated at a high membrane potential. It is catalysed by UCP3 and ANT. Although it is inhibited by GDP and carboxyatractylate, these inhibitors do not show the expected classical specificity.

Abbreviations used: ANT, adenine nucleotide translocase; TPMP, triphenylmethylphosphonium; UCP, uncoupling protein; *Ucp3*KO, *Ucp3* knockout; WT, wild-type.

[1] To whom correspondence should be addressed (email np@mrc-dunn.cam.ac.uk).

EXPERIMENTAL

Animals

Female Wistar rats (Charles River) and male or female mice were housed at 21 ± 2 °C, 57 ± 5 % humidity, 12/12 h light/dark, with standard laboratory chow and water *ad libitum*, following UK Home Office Guidelines for the Care and Use of Laboratory Animals. *Ucp3* knockout (termed *Ucp3*KO) [39] and wild-type (termed WT) sibling-paired mice were used at age 12–15 weeks. *Ucp3* ablation was confirmed by PCR analysis of genomic *Ucp3* and Western blot analysis in skeletal muscle mitochondria.

Mitochondria

Animals (one rat or four mice per preparation) were killed by stunning and cervical dislocation. Mitochondria were isolated from total hind limb skeletal muscle [15]. Mitochondria from WT and *Ucp3*KO mice were prepared and assayed in parallel.

Proton-leak kinetics

Proton-leak rates across the inner membrane of isolated mitochondria were measured as the oxygen consumption required to pump the protons back out of the mitochondrial matrix (in the presence of oligomycin to prevent ATP synthesis) [40]. Proton-leak kinetics were measured as the dependence of proton-leak rate on its driving force, protonmotive force (measured as membrane potential in the presence of nigericin to abolish pH gradients). Respiration rate and membrane potential were measured simultaneously using electrodes sensitive to oxygen or the membrane-potential-dependent probe, $TPMP^+$ (triphenylmethylphosphonium). Assay medium contained 0.35 mg/ml mitochondrial protein, 120 mM KCl, 5 mM KH_2PO_4, 3 mM Hepes, 1 mM EGTA, 0.3 % (w/v) defatted BSA (unless otherwise stated), 5 μM rotenone, 1 μg/ml oligomycin and 0.11 μM nigericin. The TPMP electrode was calibrated with sequential additions of 0.5 μM TPMP up to 2.5 μM and the mitochondria were energized with 4 mM succinate. Leak kinetics were measured by varying oxygen consumption and membrane potential by sequential additions of malonate (approx. 0.1–2.3 mM). After each run, 0.2 μM FCCP (carbonyl cyanide *p*-trifluoromethoxyphenylhydrazone) was added to release matrix TPMP, allowing correction for any small baseline drift. The TPMP-binding correction was taken to be 0.35 (μl/mg protein)$^{-1}$ [41].

Measurement of ANT content by carboxyatractylate titre

Respiration was measured without oligomycin or nigericin. In order to establish the maximum phosphorylating rate 1 mM ADP was added, and then respiration was successively inhibited by additions of carboxyatractylate (Calbiochem) until the resting non-phosphorylating rate was re-established. Carboxyatractylate binds ANT very tightly, so ANT content was interpolated as the minimum amount of carboxyatractylate required to abolish phosphorylating respiration [11,42].

Statistics

To test for differences in proton conductance by ANOVA or paired Student's *t* tests, we calculated respiration rates (by linear interpolation between flanking points) at the highest membrane potential common to all conditions on a given day. Means for each condition (± S.E.M.) are plotted in bar graphs, with the mean value of the highest common potential indicated.

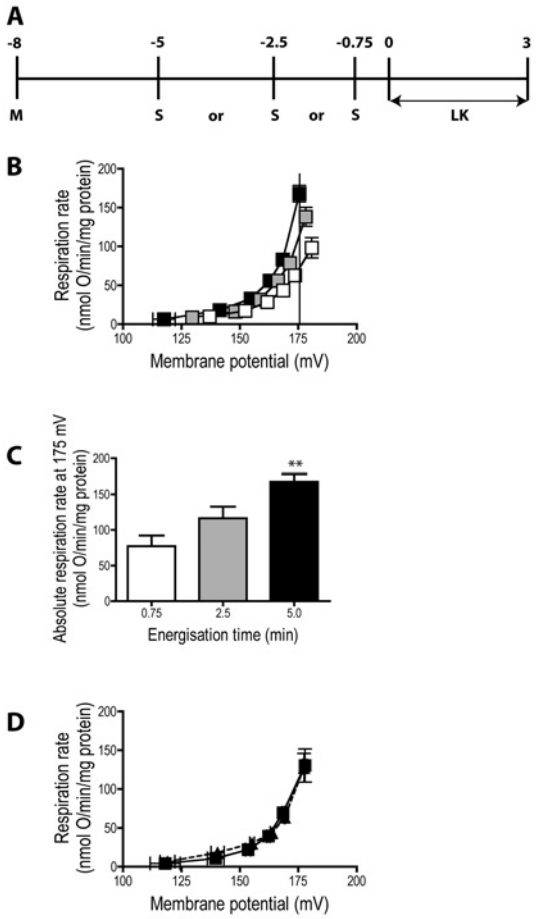

Figure 1 Energization-dependent proton conductance of rat skeletal muscle mitochondria

Proton-leak kinetics were measured in rat skeletal muscle mitochondria as described in the Experimental section. (**A**) Timings of additions to the incubation chamber. Mitochondria plus inhibitors (M) were added at $t = -8$ min, 4 mM succinate (S) was added at the times indicated, then leak kinetics (LK) were measured between $t = 0$ and $t = 3$ min by titration of membrane potential and oxygen consumption rate with malonate from 0.14 to 2.3 mM. (**B**) Kinetic response of mitochondrial proton-leak rate (measured as oxygen consumption rate) to membrane potential measured after energization with 4 mM succinate for 0.75 (open squares), 2.5 (grey squares) or 5 min (black squares). (**C**) Proton-leak rate at 175 mV [solid vertical line of (**B**)]; the average highest protonmotive force common to all curves generated in the experiment. (**D**) Comparison of proton-leak curves generated either in a single experiment using sequential malonate additions over 3 min (S at $t = -5$ min, leak kinetics measured between $t = 0$ and $t = 3$ min; squares) or in five separate experiments each with a different concentration of malonate added at $t = 0$ (S at $t = -5$ min; 0.14–2.3 mM malonate added at $t = 0$, leak kinetics measured between $t = 0$ and $t = 0.5$ min; triangles). Values are means ± S.E.M. of duplicate experiments performed on four (**B** and **C**) or three (**D**) separate preparations. One-way ANOVA was performed for (**C**); $P = 0.0034$, with Dunnett's multiple comparison test used post-hoc comparing other bars to 0.75 min: $^{**}P < 0.01$.

RESULTS

Time-dependent endogenous activation of proton conductance in energized rat skeletal muscle mitochondria

Preliminary investigations of proton-leak kinetics in skeletal muscle mitochondria suggested that proton conductance increased as the time of energization with succinate was extended. Figure 1 characterizes this endogenous activation of proton conductance. Mitochondria were incubated in assay medium for a total of 8 min (Figure 1A). They were energized with succinate for the last 0.75, 2.5 or 5 min, then proton-leak kinetics were measured. Figure 1(B) shows that respiration driving proton

leak increased as incubation with succinate was extended. To allow comparison of proton-leak rates at the same driving force, Figure 1(C) shows rates interpolated at 175 mV, the highest common membrane potential in the experiment, indicated by the vertical line. The proton-leak rate at 175 mV measured after 5 min with succinate was significantly higher than that measured after 0.75 min with succinate. The total time in the assay was always 8 min, therefore endogenous proton conductance increases as the time of incubation with succinate is extended.

Leak kinetics are measured by titrating membrane potential and respiration rate with malonate over 3 min. If time with succinate is important in inducing proton leak, endogenous activation should continue during the malonate titration, causing later points to be more uncoupled than earlier points. To test this, Figure 1(D) shows a compilation of leak kinetics measured in five separate experiments, each with a different concentration of malonate added at $t = 0$. Time with succinate was the same for all titration points (broken line). This was overlaid on the leak kinetics measured during one standard experiment using five sequential additions of malonate (as in Figure 1B), where time with succinate differed between titration points (solid line). There was no difference in leak kinetics between the two protocols. Therefore energization-dependent uncoupling does not increase over the 3 min taken to measure the proton-leak kinetics suggesting no further increases after the first malonate addition.

Malonate attenuates the energization-dependent increase in proton conductance by lowering membrane potential in rat skeletal muscle mitochondria

To test the ability of malonate to blunt energization-dependent, endogenous activation of proton leak, 430 μM malonate was added immediately before succinate. At $t = 0$, after incubation with succinate for 1.5 min, this concentration of malonate lowered the membrane potential by approx. 12 mV (X in Figure 2). Succinate was added 1.5 min or 5 min before the leak titration, which was completed as normal with sequential additions of malonate (Figure 2B). Figure 2(A) shows the control without malonate pre-addition.

To allow comparison of proton-leak rates at the same driving force, Figure 2(C) shows the time-dependent increases in rates with succinate, interpolated at the highest common membrane potential, 169 mV. The leak induced between 1.5 and 5 min was significantly lower when 430 μM malonate was present, therefore malonate does indeed attenuate the energization-dependent increase in proton conductance.

Pre-addition of malonate could inhibit energization-dependent induced leak directly, or by lowering protonmotive force, or by oxidizing the electron transport chain. To test these possibilities, the experiment in Figure 2(C) was repeated using the complex IV inhibitor, KCN, at a concentration that lowers the membrane potential to the same extent as 430 μM malonate. Leak kinetics were measured in the absence (Figure 2D) or presence (Figure 2E) of 43 μM KCN. At the highest common membrane potential, proton conductance induced by succinate between 1.5 and 5 min in the presence of 43 μM KCN (Figure 2F) was significantly lower than in its absence. Unlike malonate, KCN reduces electron transport chain intermediates. The two inhibitors decreased energization-dependent proton conductance to a similar extent, suggesting that it is high membrane potential, not a particular redox state, that is required for energization-dependent induction of proton conductance.

The increase in proton conductance between 1.5 and 5 min incubation with succinate was also measured at intermediate concentrations of pre-added malonate or KCN. This produced

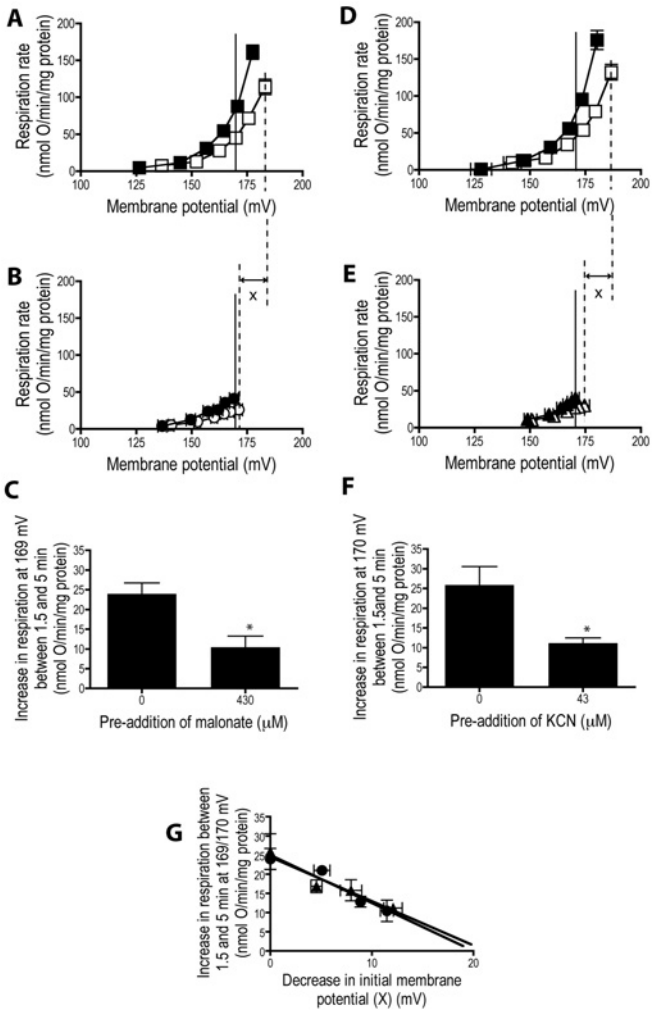

Figure 2 Sensitivity of energization-dependent proton conductance in rat skeletal muscle mitochondria to membrane potential

(**A**–**C**) Effect of malonate. (**D**–**F**) Effect of KCN. (**A**, **B**, **D** and **E**) Proton-leak kinetics. Succinate at 4 mM was added at $t = -1.5$ min (open symbols) or $t = -5$ min (closed symbols) (see Figure 1A). Proton-leak kinetics were measured between $t = 0$ and $t = 3$ min after no treatment (**A** and **D**) or addition of 430 μM malonate (**B**) or 43 μM KCN (**E**) immediately prior to addition of succinate. (**C** and **F**) Inhibition of energization-dependent proton leak by malonate and KCN. The increase in proton conductance at $t = 0$ caused by incubation with succinate between -5.0 min and -1.5 min was interpolated at the highest common membrane potential, 169 mV [solid vertical line in (**A** and **B**)] in (**C**) and 170 mV [solid vertical line in (**D** and **E**)] in (**F**). 'X' indicates the drop in membrane potential measured at $t = 0$ caused by addition of malonate or KCN prior to addition of succinate at $t = -1.5$ min. (**G**) Effect of this drop in membrane potential on energization-dependent increase in proton conductance. The increases in proton-leak rate from (**C**) and additional experiments (results not shown) using 140 μM and 290 μM malonate (circles), and from (**F**) and additional experiments (results not shown) using 14 μM and 29 μM KCN (triangles) are plotted against the drop ('X') in membrane potential at $t = 0$ after succinate addition at $t = -1.5$ min. Values are means $\pm$ S.E.M. of five (**A**–**C**) or six (**D**–**F**) experiments each performed in duplicate. $^*P < 0.03$, significantly different from no addition as measured by paired Student's t test. Lines in (**G**) are linear regressions.

intermediate drops in membrane potential at $t = 0$ following 1.5 min with succinate (equivalent to X in Figure 2B and Figure 2E). To characterize the ability of decreased membrane potential to blunt energization-dependent induction of proton conductance, Figure 2(G) shows the increase in leak rate (e.g. Figures 2C and 2F) plotted against the drop (X) in membrane potential caused by different concentrations of pre-added malonate or KCN. There was a linear decrease in activation as membrane potential during the activatory period was decreased.

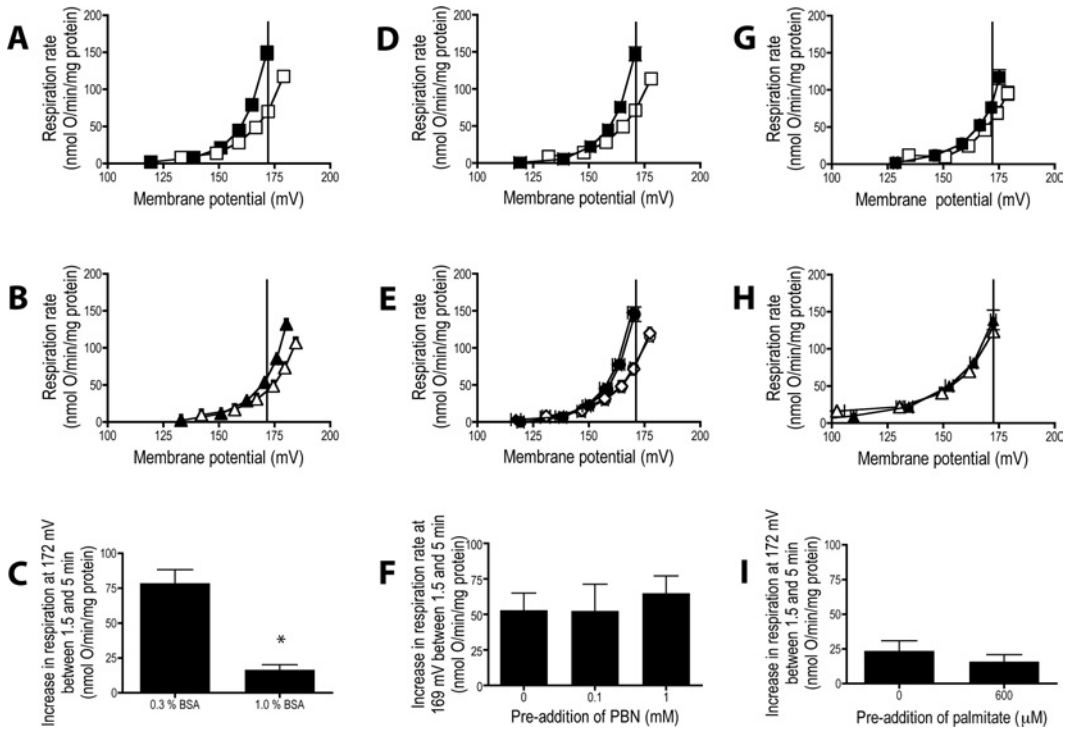

Figure 3 Modulation of energization-dependent leak in rat skeletal muscle mitochondria by BSA, phenylbutylnitrone and palmitate

(**A**–**C**) Effect of 1 % BSA. (**D**–**F**) Effect of phenylbutylnitrone (PBN). (**G**–**I**) Effect of palmitate. (**A**, **B**, **D**, **E**, **G** and **H**) Proton-leak kinetics. Succinate at 4 mM was added at $t = -1.5$ min (open symbols) or $t = -5$ min (closed symbols) (see Figure 1A). Proton-leak kinetics were measured between $t = 0$ and $t = 3$ min in medium containing 0.3 % (**A** and **D**) or 1 % (w/v) BSA (**B**, **G** and **H**), after no pre-treatment or pre-treatment with 0.1 mM (triangles) or 1 mM phenylbutylnitrone (diamonds) (**E**) or 600 μM palmitate (**H**). (**C**, **F** and **I**) Effect on energization-dependent proton leak of 1 % BSA, phenylbutylnitrone or palmitate. The increase in proton conductance at $t = 0$ caused by incubation with succinate between -5 and -1.5 min was interpolated at the highest common membrane potential, 172 mV [solid vertical line in (**A**, **B**, **G** and **H**)] in (**C**) and (**I**) and 169 mV [solid vertical line in (**D** and **E**)] in (**F**). Values are means $\pm$ S.E.M. of four (**A**–**C**), three (**D**–**F**) or three (**G**–**I**) experiments, each performed in duplicate. * $P < 0.01$, significantly different from 0.3 % BSA as measured by paired Student's t test.

The linear regressions for malonate and KCN overlap, suggesting a conserved mechanism of inhibition through the lowering of membrane potential. Extrapolation to zero effect suggests that a decrease of 20 mV is sufficient to prevent activation of proton conductance.

Therefore the endogenous energization-dependent activation of proton conductance following addition of succinate requires a high membrane potential. Activation increases over 5 min with succinate but during subsequent titrations with malonate the membrane potential falls by more than 20 mV and further activation is prevented.

What is the activator of the energization-dependent increase in proton conductance in rat skeletal muscle mitochondria?

BSA removes putative endogenous activators, including fatty acids [43] and reactive oxygen species [6] and their derivatives such as reactive alkenals [15]. To test whether these endogenous activators were involved in the observed energization-dependent proton leak, the concentration of BSA was increased in the standard assay medium from 0.3 % to 1 % (w/v) (Figures 3A–3C). Proton-leak kinetics were measured after energization with succinate for 1.5 or 5 min in the presence of 0.3 % (Figure 3A) or 1 % (Figure 3B) BSA. At 172 mV, leak induced between 1.5 and 5 min in assay medium containing 1 % BSA was significantly lower than in 0.3 % BSA (Figure 3C), showing that BSA blunts energization-dependent activation of proton conductance and suggesting that an endogenous activator that is quenched by BSA mediates the induced leak.

To test the possibility that the increase in energization-dependent leak is due to lipid peroxidation products, phenylbutylnitrone, a chain-breaking spin trap that quenches carbon-centred radical intermediates, was pre-added to the assay medium at concentrations known to inhibit lipid peroxidation [44]. Proton-leak kinetics were measured after energization with succinate for 1.5 or 5 min in the absence (Figure 3D) or presence (Figure 3E) of phenylbutylnitrone. At 169 mV, there was no significant effect of phenylbutylnitrone on leak induced between 1.5 and 5 min (Figure 3F), suggesting that pathways that generate lipid peroxidation products through a carbon-centred radical sensitive to phenylbutylnitrone are not involved in the energization-dependent uncoupling. However, other reactive oxygen species-related activators remain candidates.

Energization might either generate a pool of activator, or allow activation of uncoupling using a pre-existing activator pool (e.g. through an energization-dependent change in conformation of an UCP). To distinguish between these alternatives, we tested the effect of pre-addition of fatty acids in medium containing 1 % BSA. Proton-leak kinetics were measured in 1 % BSA in the absence (Figure 3G) or presence (Figure 3H) of 600 μM palmitate after energization with succinate for 1.5 or 5 min. Figure 3(I) replicates the observation in Figure 3(C) that 1 % BSA alone prevented time-dependent activation. Pre-addition of palmitate did not overcome the inhibitory effect of 1 % BSA, showing that time-dependent activation did not occur by potential-dependent changes in protein conformation that then allowed activation by a pre-existing pool of fatty acids. Fatty acids remain, however, one candidate for the endogenously generated activator, since

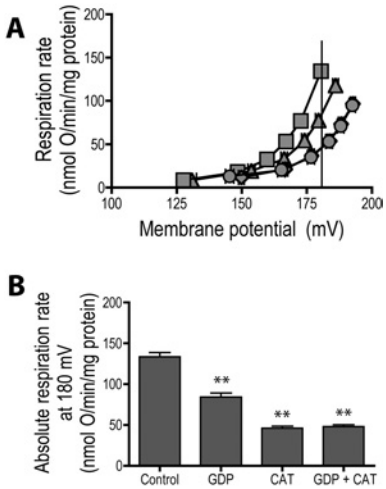

Figure 4 Inhibition of proton conductance in rat skeletal muscle mitochondria by GDP and carboxyatractylate

(**A**) Proton-leak kinetics measured between $t = 0$ and $t = 3$ min following addition of inhibitors (where present) and mitochondria at $t = -5.5$ min. Succinate at 4 mM was added at $t = -2.5$ min (see Figure 1A) in the presence of no additions (squares), 500 μM GDP (triangles), 2.5 μM carboxyatractylate (diamonds) or GDP and carboxyatractylate (circles). (**B**) Absolute respiration rate at 180 mV [solid vertical line in (**A**)] in each condition. Values are means $\pm$ S.E.M. of 15 experiments, each performed in duplicate. One-way ANOVA was performed for (**B**); $P = 0.0001$, with Dunnett's multiple comparison test used post-hoc comparing other bars to control: $^{**}P < 0.01$.

proton-leak kinetics in the presence of palmitate (Figure 3H) were the same after 1.5 min incubation with succinate as those seen in 0.3 % BSA after 5 min with succinate (Figure 3A).

These experiments are consistent with at least three different interpretations. The endogenous activator may be (i) fatty acids, (ii) some other molecule, generated during 5 min incubation at high membrane potential, or (iii) some molecule (e.g. hydroxynonenal) that is already present in the mitochondria before addition of succinate, but requires the membrane potential to be high for several minutes to allow the interaction that causes uncoupling.

Which proteins catalyse the energization-dependent increase in proton conductance in rat skeletal muscle mitochondria?

Uncoupling through the ANT is inhibited by carboxyatractylate [13], whereas uncoupling through UCPs is classically inhibited by GDP [14,45]. Proton-leak kinetics were measured after energization with succinate for 2.5 min in the absence and presence of carboxyatractylate and GDP to determine whether ANT and UCP3 were involved (Figure 4A). Figure 4(B) shows that at the highest common membrane potential, 180 mV, GDP and carboxyatractylate significantly inhibited proton conductance separately and in combination. The extent of the carboxyatractylate inhibition of proton conductance suggests that the majority is attributable to ANT. As observed previously [15], inhibition of proton conductance by GDP and carboxyatractylate was non-additive; characterization of the relative contributions of ANT and UCP3 therefore required further experiments.

UCP3 and ANT each catalyse part of the energization-dependent increase in proton conductance in mouse skeletal muscle mitochondria

The contribution of UCP3 to energization-dependent proton conductance was assessed using skeletal muscle mitochondria prepared from WT and *Ucp3*KO mice. Proton-leak kinetics were

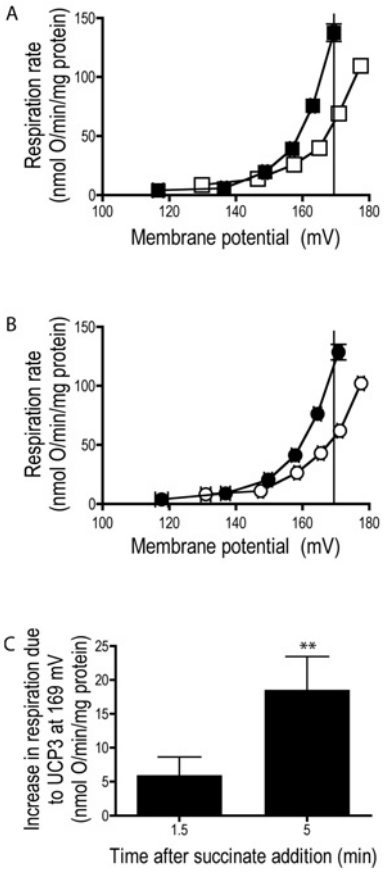

Figure 5 Contribution of UCP3 and ANT to energization-dependent leak in mouse skeletal muscle mitochondria

(**A** and **B**) Proton-leak kinetics. (**A**) Mitochondria from WT mice. (**B**) Mitochondria from *Ucp3*KO mice. Succinate at 4 mM was added at $t = -1.5$ min (open symbols) or $t = -5$ min (closed symbols) (see Figure 1A). (**C**) Proton leak due to UCP3 measured at 169 mV [solid vertical line in (**A** and **B**)] as (**A**) minus (**B**). Values are means $\pm$ S.E.M. of seven experiments, each performed in duplicate. $^{**}P < 0.01$, significantly different by paired Student's t test (5 min succinate addition compared with 1.5 min).

measured after energization with succinate for 1.5 or 5 min. Figure 5(A) shows that skeletal muscle mitochondria from WT mice showed a similar time-dependent increase in proton leak after addition of succinate to mitochondria from rat (Figure 1B). Figure 5(B) shows the same experiment performed using skeletal muscle mitochondria from *Ucp3*KO mice. There was still a difference between the curves, but it was smaller than in WT. The difference is quantified in Figure 5(C), which shows proton leak through UCP3, expressed as the difference between rates in skeletal muscle mitochondria from WT and *Ucp3*KO mice at 169 mV. UCP3-associated proton conductance was significantly greater after incubation with succinate for 5 min than for 1.5 min. In the presence of UCP3, the increase in respiration rate between 1.5 and 5 min was 75 nmol of O/min per mg of protein whereas in the absence of UCP3 it was 62 nmol of O/min per mg of protein. Thus approx. 17 % of the energization-dependent proton leak induced between 1.5 and 5 min incubation with succinate requires the presence of UCP3.

The contribution of ANT to the proton conductance observed after 5 min incubation with succinate was assessed as the carboxyatractylate-sensitive effect in skeletal muscle mitochondria from *Ucp3*KO mice. Figure 6(B) shows that carboxyatractylate substantially inhibited energization-dependent proton conductance

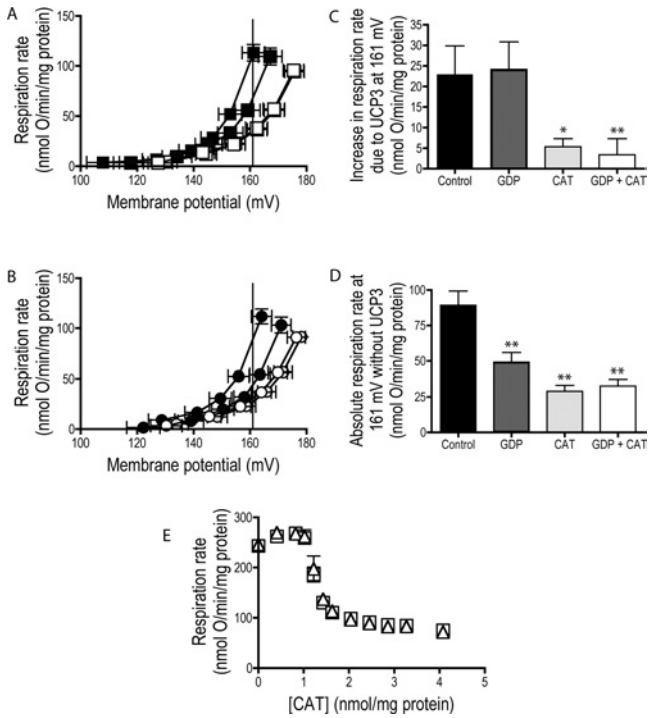

Figure 6 Inhibition of proton conductance in skeletal muscle mitochondria from *Ucp3*WT and *Ucp3*KO mice by GDP and carboxyatractylate

(**A** and **B**) Proton-leak kinetics. (**A**) Mitochondria from WT mice. (**B**) Mitochondria from *Ucp*3KO mice. Succinate at 4 mM was added at $t = -5$ min (see Figure 1A). Proton-leak kinetics were measured after 5 min incubation with 4 mM succinate in the absence (closed symbols) or presence of 500 μM GDP (dark grey symbols), 2.5 μM carboxyatractylate (light grey symbols) or GDP and carboxyatractylate (open symbols). (**C**) Proton leak due to UCP3 measured at 161 mV [solid vertical line in (**A** and **B**)] as (**A**) minus (**B**). (**D**) Proton leak not due to UCP3 measured at 161 mV, data from (**B**). (**E**) Carboxyatractylate titration of ANT content in mitochondria from WT mice (squares) and *Ucp3*KO mice (triangles). Values are means $\pm$ S.E.M. of ten (**A**–**D**) and four (**E**) experiments, each performed in duplicate. One-way ANOVA was performed for (**C**) and (**D**); $P = 0.0001$, with Dunnett's multiple comparison test used post-hoc comparing other bars to control: $^{*}P < 0.05$; $^{**}P < 0.01$.

in the absence of UCP3. The effect is quantified in Figure 6(D), which shows UCP3-independent leak at 161 mV. Carboxyatractylate lowered the rate from 90 to 30 nmol of O/min per mg of protein, equivalent to approx. 50–55 % of the total effect in mitochondria from WT mice in Figure 6(A). Together, these results show that the energization-dependent proton conductance in mouse skeletal muscle mitochondria is catalysed approx. 15–20 % by UCP3, 50–55 % by ANT and 25–30 % by other pathways not sensitive to GDP or carboxyatractylate (e.g. the dicarboxylate carrier).

Specificity and lack of additivity of inhibition by GDP and carboxyatractylate in mouse skeletal muscle mitochondria

To investigate the lack of additivity between the inhibitors GDP and carboxyatractylate in rat skeletal muscle (Figure 4), and also seen in other studies [15], inhibition was measured in skeletal muscle mitochondria from WT and *Ucp3*KO mice. The same lack of additivity was seen in skeletal muscle mitochondria from WT mice (Figure 6A) as in rat: GDP partially inhibited proton conductance in the absence of carboxyatractylate but caused no further inhibition in the presence of carboxyatractylate. Figure 6(B) shows the same effect in mitochondria from *Ucp3*KO mice.

Figures 6(C) and 6(D) dissect out the effects of the inhibitors. Figure 6(C) represents the contribution of UCP3 (Figure 6A minus 6B) at the highest common membrane potential, 161 mV, after 5 min incubation with succinate. Surprisingly (since GDP is the classical inhibitor of UCPs), the proton conductance through UCP3 under these conditions was insensitive to GDP. More surprisingly (since carboxyatractylate is thought to be a highly specific inhibitor of ANT), it was almost fully sensitive to carboxyatractylate. This sensitivity of UCP3 to carboxyatractylate partially explains the lack of additivity of the two inhibitors: once UCP3 is inhibited by carboxyatractylate, any inhibition by GDP would have no further effect.

Figure 6(D) represents the contribution of ANT and other pathways (results from Figure 6B). The energization-dependent proton conductance of mitochondria from *Ucp3*KO mice was significantly lower in the presence of GDP, indicating that an endogenously activated pathway other than UCP3 was inhibited by GDP. Since this conductance was also strongly inhibited by carboxyatractylate, it was catalysed by ANT. This experiment shows that GDP is not specific for UCPs, but can also inhibit proton conductance through other pathways, specifically ANT. It completes the explanation of the lack of additivity of GDP and carboxyatractylate: once ANT is inhibited by carboxyatractylate, inhibition by GDP would have no further effect. Together, these results highlight potential promiscuity of the inhibitors GDP and carboxyatractylate: neither is specific for its classical target in our experiments.

A possible alternative explanation of the sensitivity of mitochondria from *Ucp3*KO mice to GDP is that the *Ucp3*KO targeting vector upregulates *Ucp2* expression, due to proximity of the *Ucp2* and *Ucp3* genes [46], and it is this UCP2 that is inhibited by GDP. We detected *Ucp2* transcript in total hind limb skeletal muscle using real-time PCR, but at levels 30 times lower than in spleen or lung, with no significant difference between WT and *Ucp3*KO (results not shown). UCP2 was undetectable by Western blot analysis using skeletal muscle mitochondria (20 μg of protein) from either WT or *Ucp3*KO mice. The antibody can detect 125 pg of affinity-purified recombinant UCP2, so UCP2 content is below 6 ng/mg of mitochondrial protein, less than 5 % of the UCP3 content of 140 ng/mg of protein in mouse skeletal muscle mitochondria [47]. UCP1 is not expressed in skeletal muscle of WT or *Ucp3*KO mice [48]. Therefore the putative presence of UCP1 or UCP2 does not explain the sensitivity of proton conductance in skeletal muscle mitochondria from *Ucp3*KO mice to GDP.

A possible alternative explanation of the decreased effect of carboxyatractylate in mitochondria from *Ucp3*KO mice is that ablation of UCP3 somehow decreased ANT content. We tested this possibility by titrating ANT activity with carboxyatractylate in skeletal muscle mitochondria from WT and *Ucp3*KO mice. UCP3 (4 pmol/mg of mitochondrial protein [47]) is approx. 0.2 % as abundant as ANT (2 nmol/mg of mitochondrial protein [11]), so any sequestering of carboxyatractylate by UCP3 would be negligible. ANT content was not significantly different (WT, 1.52 nmol/mg of protein and *Ucp3*KO, 1.56 nmol/mg of protein; Figure 6E), eliminating this explanation.

Inhibition of UCP3 by carboxyatractylate could be direct or through ANT. To examine this, we tested the effects of an alternative ANT inhibitor, bongkrekate. Unlike carboxyatractylate, which binds to the *C* conformation of the carrier, bongkrekate binds to the *M* conformation [49]. BSA was omitted from the assay medium because it binds bongkrekate. Proton-leak kinetics were measured in skeletal muscle mitochondria isolated from WT (Figure 7A) and *Ucp3*KO (Figure 7B) mice after energization with succinate for 5 min in the absence or presence

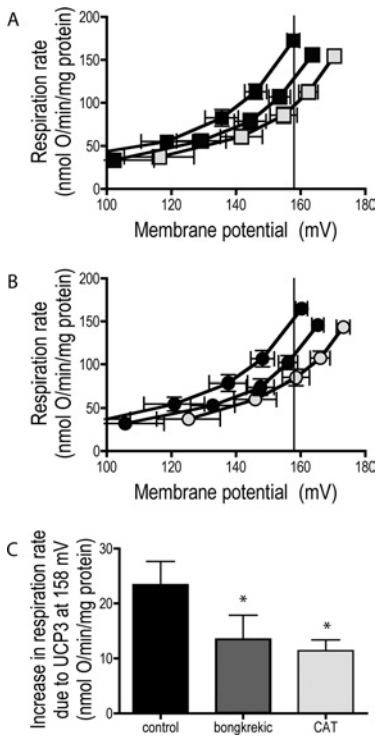

Figure 7 Inhibition of proton conductance in *Ucp3*WT and *Ucp3*KO mouse skeletal muscle mitochondria by carboxyatractylate and bongkrekate

(**A** and **B**) Proton-leak kinetics. (**A**) Mitochondria from WT mice. (**B**) Mitochondria from *Ucp3*KO mice. Succinate at 4 mM was added at $t = -5$ min (see Figure 1A) in the absence of BSA in the absence (closed symbols) or presence of 2.0 μM bongkrekate (dark grey) or 2.5 μM carboxyatractylate (light grey). (**C**) Proton leak due to UCP3 measured at 158 mV [solid vertical line in (**A** and **B**)] as (**A**) minus (**B**). Values are means $\pm$ S.E.M. of ten experiments, each performed in duplicate. One-way ANOVA was performed for (**C**); $P = 0.015$, with Dunnett's multiple comparison test used post-hoc comparing other bars with control: $^*P < 0.05$.

of bongkrekate or carboxyatractylate. Bongkrekate partially inhibited the energization-dependent proton conductance in both cases. Figure 7(C) shows the effects that were dependent on UCP3 (Figure 7A minus 7B). At the highest common membrane potential, 158 mV, both carboxyatractylate and bongkrekate inhibited proton conductance through UCP3. It is unlikely that UCP3 and ANT share two different high-affinity inhibitor sites, therefore both carboxyatractylate and bongkrekate act on the UCP3-associated leak indirectly through primary effects on ANT.

DISCUSSION

In the present study we describe an endogenous activation of the proton conductance of skeletal muscle mitochondria isolated from both rats and mice that increases with time after energization. This effect is not dependent upon redox state but requires a high membrane potential upon succinate addition. The effect of membrane potential may be to increase the production of endogenous fatty acids or other molecules that progressively activate uncoupling, or to sensitize target proteins to the effects of generated or pre-existing activators such as products of reactive oxygen species. The mechanism remains unclear. Membrane potential might change the conformation of membrane lipids to facilitate access by phospholipases, or might change the conformations of UCP3 and ANT to expose activator-binding sites. Mobilization of fatty acids could explain the lack of GDP sensitivity of the UCP3-dependent proton conductance, by analogy with UCP1, where fatty acids functionally compete with inhibitory nucleotides [50]. Whatever the activator and mechanism, energization-dependent uncoupling of skeletal muscle mitochondria may be important in limiting membrane potential during rest, to limit reactive oxygen species production [21] or prevent dielectric breakdown of the membrane [4].

Two catalysts of energization-dependent proton conductance were found to be UCP3 and ANT. In WT mouse skeletal muscle mitochondria after 5 min incubation with succinate, the relative contributions of UCP3, ANT and other pathways to proton conductance were 15–20 %, 50–55 % and 25–30 % respectively. Since UCP3 content is only approx. 0.2 % of ANT content (see above), this result demonstrates that the specific proton flux through UCP3 is 100–200 times greater than that through ANT. The greater specific activity of UCP3 may allow finer control of high membrane potential in tissues that contain this protein in addition to ANT.

We found that GDP partially inhibited the contribution of ANT to energization-dependent proton conductance. Khailova et al. [51] also concluded that GDP inhibits proton translocation by ANT, although they did not use *Ucp* knockout controls, which provide our most compelling evidence that GDP can inhibit proton conductance in the absence of UCP3. GDP and GTP bind weakly to ANT [52], but compete poorly with ADP and ATP, so they are not regarded as inhibitors of adenine nucleotide exchange. However, adenine nucleotides are absent in assays of proton conductance, which may allow guanine nucleotides to bind and partially inhibit ANT-catalysed proton leak.

We found that carboxyatractylate inhibited the contribution of UCP3 to proton leak. Carboxyatractylate is a high-affinity inhibitor of ANT, and has not been shown previously to act on other proteins. However, most other studies have not looked for carboxyatractylate inhibition of UCP3 function. The observation that bongkrekate also inhibits UCP3-dependent proton conductance suggests that inhibition of UCP3 is indirect, via primary effects on ANT. It is unclear what these indirect effects might be, but they might involve protein–protein interactions between ANT and UCP3, or interactions through some other protein, lipid or small molecule. More exploration of the interaction is required to uncover the mechanism. However, the (indirect) inhibition of UCP3 by carboxyatractylate fully explains the hitherto puzzling lack of additivity between inhibition of proton conductance by GDP and carboxyatractylate.

Since inhibition by GDP and carboxyatractylate is also non-additive in mitochondria from kidney [15,44], carboxyatractylate may also inhibit UCP2 by a similar indirect mechanism. However, it appears that carboxyatractylate does not inhibit potato UCP [53] or mammalian UCP1, since guanine nucleotides are still inhibitory in the presence of carboxyatractylate in mitochondria from potato or mammalian brown adipose tissue. Thus caution should be shown when using sensitivity to GDP or carboxyatractylate as diagnostic of the involvement of a UCP or ANT in proton conductance. Observations of GDP or carboxyatractylate sensitivity should be verified by independent assays of the involvement of UCPs and ANT, such as sensitivity to genetic ablation or overexpression.

We thank Dr Mary-Ellen Harper (Ottawa) for *Ucp3*KO mice and Julie Buckingham and Helen Boysen for technical assistance. This work was supported by the Medical Research Council and the Wellcome Trust (grants 065326/Z/01/Z and 066750/B/01/Z).

REFERENCES

1 Brand, M. D. (1990) The proton leak across the mitochondrial inner membrane. Biochim. Biophys. Acta **1018**, 128–133

2 Brand, M. D., Chien, L. F., Ainscow, E. K., Rolfe, D. F. S. and Porter, R. K. (1994) The causes and functions of mitochondrial proton leak. Biochim. Biophys. Acta **1187**, 132–139

3 Rolfe, D. F. S. and Brand, M. D. (1996) Contribution of mitochondrial proton leak to skeletal muscle respiration and to standard metabolic rate. Am. J. Physiol. **271**, C1380–C1389

4 Rolfe, D. F. S. and Brand, M. D. (1997) The physiological significance of mitochondrial proton leak in animal cells and tissues. Biosci. Rep. **17**, 9–16

5 Rolfe, D. F. S., Newman, J. M., Buckingham, J. A., Clark, M. G. and Brand, M. D. (1999) Contribution of mitochondrial proton leak to respiration rate in working skeletal muscle and liver and to SMR. Am. J. Physiol. **276**, C692–C699

6 Echtay, K. S., Murphy, M. P., Smith, R. A., Talbot, D. A. and Brand, M. D. (2002) Superoxide activates mitochondrial uncoupling protein 2 from the matrix side. Studies using targeted antioxidants. J. Biol. Chem. **277**, 47129–47135

7 Affourtit, C. and Brand, M. D. (2008) Uncoupling protein-2 contributes significantly to high mitochondrial proton leak in INS-1E insulinoma cells and attenuates glucose-stimulated insulin secretion. Biochem. J. **409**, 199–204

8 Dilger, J. P., McLaughlin, S. G., McIntosh, T. J. and Simon, S. A. (1979) The dielectric constant of phospholipid bilayers and the permeability of membranes to ions. Science **206**, 1196–1198

9 Brookes, P. S., Rolfe, D. F. S. and Brand, M. D. (1997) The proton permeability of liposomes made from mitochondrial inner membrane phospholipids: comparison with isolated mitochondria. J. Membr. Biol. **155**, 167–174

10 Brown, G. C. and Brand, M. D. (1991) On the nature of the mitochondrial proton leak. Biochim. Biophys. Acta **1059**, 55–62

11 Brand, M. D., Pakay, J. L., Ocloo, A., Kokoszka, J., Wallace, D. C., Brookes, P. S. and Cornwall, E. J. (2005) The basal proton conductance of mitochondria depends on adenine nucleotide translocase content. Biochem. J. **392**, 353–362

12 Andreyev, A., Bondareva, T. O., Dedukhova, V. I., Mokhova, E. N., Skulachev, V. P., Tsofina, L. M., Volkov, N. I. and Vygodina, T. V. (1989) The ATP/ADP-antiporter is involved in the uncoupling effect of fatty acids on mitochondria. Eur. J. Biochem. **182**, 585–592

13 Andreyev, A., Bondareva, T. O., Dedukhova, V. I., Mokhova, E. N., Skulachev, V. P. and Volkov, N. I. (1988) Carboxyatractylate inhibits the uncoupling effect of free fatty acids. FEBS Lett. **226**, 265–269

14 Cadenas, S., Buckingham, J. A., St-Pierre, J., Dickinson, K., Jones, R. B. and Brand, M. D. (2000) AMP decreases the efficiency of skeletal-muscle mitochondria. Biochem. J. **351**, 307–311

15 Echtay, K. S., Esteves, T. C., Pakay, J. L., Jekabsons, M. B., Lambert, A. J., Portero-Otin, M., Pamplona, R., Vidal-Puig, A. J., Wang, S., Roebuck, S. J. and Brand, M. D. (2003) A signalling role for 4-hydroxy-2-nonenal in regulation of mitochondrial uncoupling. EMBO J. **22**, 4103–4110

16 Samartsev, V. N., Smirnov, A. V., Zeldi, I. P., Markova, O. V., Mokhova, E. N. and Skulachev, V. P. (1997) Involvement of aspartate/glutamate antiporter in fatty acid-induced uncoupling of liver mitochondria. Biochim. Biophys. Acta **1319**, 251–257

17 Engstova, H., Zackova, M., Ruzicka, M., Meinhardt, A., Hanus, J., Kramer, R. and Jezek, P. (2001) Natural and azido fatty acids inhibit phosphate transport and activate fatty acid anion uniport mediated by the mitochondrial phosphate carrier. J. Biol. Chem. **276**, 4683–4691

18 Echtay, K. S., Pakay, J. L., Esteves, T. C. and Brand, M. D. (2005) Hydroxynonenal and uncoupling proteins: a model for protection against oxidative damage. Biofactors **24**, 119–130

19 Brand, M. D. and Esteves, T. C. (2005) Physiological functions of the mitochondrial uncoupling proteins UCP2 and UCP3. Cell Metab. **2**, 85–93

20 Esteves, T. C. and Brand, M. D. (2005) The reactions catalysed by the mitochondrial uncoupling proteins UCP2 and UCP3. Biochim. Biophys. Acta **1709**, 35–44

21 Brand, M. D., Affourtit, C., Esteves, T. C., Green, K., Lambert, A. J., Miwa, S., Pakay, J. L. and Parker, N. (2004) Mitochondrial superoxide: production, biological effects, and activation of uncoupling proteins. Free Radical Biol. Med. **37**, 755–767

22 Rafael, J., Ludolph, H. J. and Hohorst, H. J. (1969) Mitochondria from brown adipose tissue: uncoupling of respiratory chain phosphorylation by long fatty acids and recoupling by guanosine triphosphate. Hoppe Seylers Z Physiol. Chem. **350**, 1121–1131

23 Echtay, K. S., Roussel, D., St-Pierre, J., Jekabsons, M. B., Cadenas, S., Stuart, J. A., Harper, J. A., Roebuck, S. J., Morrison, A., Pickering, S. et al. (2002) Superoxide activates mitochondrial uncoupling proteins. Nature **415**, 96–99

24 Esteves, T. C., Parker, N. and Brand, M. D. (2006) Synergy of fatty acid and reactive alkenal activation of proton conductance through uncoupling protein 1 in mitochondria. Biochem. J. **395**, 619–628

25 Rial, E., Gonzalez-Barroso, M., Fleury, C., Iturrizaga, S., Sanchis, D., Jimenez-Jimenez, J., Ricquier, D., Goubern, M. and Bouillaud, F. (1999) Retinoids activate proton transport by the uncoupling proteins UCP1 and UCP2. EMBO J. **18**, 5827–5833

26 Fleury, C., Neverova, M., Collins, S., Raimbault, S., Champigny, O., Levi-Meyrueis, C., Bouillaud, F., Seldin, M. F., Surwit, R. S., Ricquier, D. and Warden, C. H. (1997) Uncoupling protein-2: a novel gene linked to obesity and hyperinsulinemia. Nat. Genet. **15**, 269–272

27 Boss, O., Samec, S., Paoloni-Giacobino, A., Rossier, C., Dulloo, A., Seydoux, J., Muzzin, P. and Giacobino, J. P. (1997) Uncoupling protein-3: a new member of the mitochondrial carrier family with tissue-specific expression. FEBS Lett. **408**, 39–42

28 Vidal-Puig, A., Solanes, G., Grujic, D., Flier, J. S. and Lowell, B. B. (1997) UCP3: an uncoupling protein homologue expressed preferentially and abundantly in skeletal muscle and brown adipose tissue. Biochem. Biophys. Res. Commun. **235**, 79–82

29 Echtay, K. S., Winkler, E., Frischmuth, K. and Klingenberg, M. (2001) Uncoupling proteins 2 and 3 are highly active H^+ transporters and highly nucleotide sensitive when activated by coenzyme Q (ubiquinone). Proc. Natl. Acad. Sci. U.S.A. **98**, 1416–1421

30 Jaburek, M., Varecha, M., Gimeno, R. E., Dembski, M., Jezek, P., Zhang, M., Burn, P., Tartaglia, L. A. and Garlid, K. D. (1999) Transport function and regulation of mitochondrial uncoupling proteins 2 and 3. J. Biol. Chem. **274**, 26003–26007

31 Dejean, L., Camara, Y., Sibille, B., Solanes, G. and Villarroya, F. (2004) Uncoupling protein-3 sensitizes cells to mitochondrial-dependent stimulus of apoptosis. J. Cell. Physiol. **201**, 294–304

32 Nadtochiy, S. M., Tompkins, A. J. and Brookes, P. S. (2006) Different mechanisms of mitochondrial proton leak in ischaemia/reperfusion injury and preconditioning: implications for pathology and cardioprotection. Biochem. J. **395**, 611–618

33 Carroll, A. M., Haines, L. R., Pearson, T. W., Fallon, P. G., Walsh, C. M., Brennan, C. M., Breen, E. P. and Porter, R. K. (2005) Identification of a functioning mitochondrial uncoupling protein 1 in thymus. J. Biol. Chem. **280**, 15534–15543

34 Ruzicka, M., Skobisova, E., Dlaskova, A., Santorova, J., Smolkova, K., Spacek, T., Zackova, M., Modriansky, M. and Jezek, P. (2005) Recruitment of mitochondrial uncoupling protein UCP2 after lipopolysaccharide induction. Int. J. Biochem. Cell Biol. **37**, 809–821

35 Fridell, Y. W., Sanchez-Blanco, A., Silvia, B. A. and Helfand, S. L. (2004) Functional characterization of a *Drosophila* mitochondrial uncoupling protein. J. Bioenerg. Biomembr. **36**, 219–228

36 Czarna, M. and Jarmuszkiewicz, W. (2005) Activation of alternative oxidase and uncoupling protein lowers hydrogen peroxide formation in amoeba *Acanthamoeba castellanii* mitochondria. FEBS Lett. **579**, 3136–3140

37 Talbot, D. A., Duchamp, C., Rey, B., Hanuise, N., Rouanet, J. L., Sibille, B. and Brand, M. D. (2004) Uncoupling protein and ATP/ADP carrier increase mitochondrial proton conductance after cold adaptation of king penguins. J. Physiol. **558**, 123–135

38 Hourton-Cabassa, C., Mesneau, A., Miroux, B., Roussaux, J., Ricquier, D., Zachowski, A. and Moreau, F. (2002) Alteration of plant mitochondrial proton conductance by free fatty acids. Uncoupling protein involvement. J. Biol. Chem. **277**, 41533–41538

39 Gong, D. W., Monemdjou, S., Gavrilova, O., Leon, L. R., Marcus-Samuels, B., Chou, C. J., Everett, C., Kozak, L. P., Li, C., Deng, C., Harper, M. E. and Reitman, M. L. (2000) Lack of obesity and normal response to fasting and thyroid hormone in mice lacking uncoupling protein-3. J. Biol. Chem. **275**, 16251–16257

40 Rolfe, D. F. S., Hulbert, A. J. and Brand, M. D. (1994) Characteristics of mitochondrial proton leak and control of oxidative phosphorylation in the major oxygen-consuming tissues of the rat. Biochim. Biophys. Acta **1188**, 405–416

41 Brand, M. D. (1995) Measurement of mitochondrial protonmotive force. In Bioenergetics: A Practical Approach (Brown, G. C. and Cooper, C. E., eds), pp. 39–62, IRL Press, Oxford, U.K.

42 Streicher-Scott, J., Lapidus, R. and Sokolove, P. M. (1993) Use of carboxyatractylate and tight-binding inhibitor theory to determine the concentration of functional mitochondrial adenine nucleotide translocators in a reconstituted system. Anal. Biochem. **210**, 69–76

43 Mellors, A., Tappel, A. L., Sawant, P. L. and Desai, I. D. (1967) Mitochondrial swelling and uncoupling of oxidative phosphorylation by lysosomes. Biochim. Biophys. Acta **143**, 299–309

44 Murphy, M. P., Echtay, K. S., Blaikie, F. H., Asin-Cayuela, J., Cocheme, H. M., Green, K., Buckingham, J. A., Taylor, E. R., Hurrell, F., Hughes, G. et al. (2003) Superoxide activates uncoupling proteins by generating carbon-centered radicals and initiating lipid peroxidation: studies using a mitochondria-targeted spin trap derived from α-phenyl-N-tert-butylnitrone. J. Biol. Chem. **278**, 48534–48545

45 Nicholls, D. G. (1976) Hamster brown-adipose-tissue mitochondria. Purine nucleotide control of the ion conductance of the inner membrane, the nature of the nucleotide binding site. Eur. J. Biochem. **62**, 223–228

46 Solanes, G., Vidal-Puig, A., Grujic, D., Flier, J. S. and Lowell, B. B. (1997) The human uncoupling protein-3 gene. Genomic structure, chromosomal localization, and genetic basis for short and long form transcripts. J. Biol. Chem. **272**, 25433–25436
47 Harper, J. A., Stuart, J. A., Jekabsons, M. B., Roussel, D., Brindle, K. M., Dickinson, K., Jones, R. B. and Brand, M. D. (2002) Artifactual uncoupling by uncoupling protein 3 in yeast mitochondria at the concentrations found in mouse and rat skeletal-muscle mitochondria. Biochem. J. **361**, 49–56
48 Vidal-Puig, A. J., Grujic, D., Zhang, C. Y., Hagen, T., Boss, O., Ido, Y., Szczepanik, A., Wade, J., Mootha, V., Cortright, R. et al. (2000) Energy metabolism in uncoupling protein 3 gene knockout mice. J. Biol. Chem. **275**, 16258–16266
49 Kramer, R. and Klingenberg, M. (1979) Reconstitution of adenine nucleotide transport from beef heart mitochondria. Biochemistry **18**, 4209–4215
50 Shabalina, I. G., Jacobsson, A., Cannon, B. and Nedergaard, J. (2004) Native UCP1 displays simple competitive kinetics between the regulators purine nucleotides and fatty acids. J. Biol. Chem. **279**, 38236–38248
51 Khailova, L. S., Prikhodko, E. A., Dedukhova, V. I., Mokhova, E. N., Popov, V. N. and Skulachev, V. P. (2006) Participation of ATP/ADP antiporter in oleate- and oleate hydroperoxide-induced uncoupling suppressed by GDP and carboxyatractylate. Biochim. Biophys. Acta **1757**, 1324–1329
52 Huber, T., Klingenberg, M. and Beyer, K. (1999) Binding of nucleotides by the mitochondrial ADP/ATP carrier as studied by 1H nuclear magnetic resonance spectroscopy. Biochemistry **38**, 762–769
53 Smith, A. M., Ratcliffe, R. G. and Sweetlove, L. J. (2004) Activation and function of mitochondrial uncoupling protein in plants. J. Biol. Chem. **279**, 51944–51952

Received 3 January 2008/30 January 2008; accepted 6 February 2008
Published as BJ Immediate Publication 6 February 2008, doi:10.1042/BJ20080006